Comparative study of approaches based on the differential critical region and correlation functions in modeling phase-transformation kinetics

Massimo Tomellini*
Dipartimento di Scienze e Tecnologie Chimiche, Università di Roma Tor Vergata, Via della Ricerca Scientifica, 00133 Roma, Italy

Massimo Fanfoni
Dipartimento di Fisica, Università di Roma Tor Vergata, Via della Ricerca Scientifica, 00133 Roma, Italy
(Received 30 July 2014; revised manuscript received 17 October 2014; published 20 November 2014)

The statistical methods exploiting the "Correlation-Functions" or the "Differential-Critical-Region" are both suitable for describing phase transformation kinetics ruled by nucleation and growth. We present a critical analysis of these two approaches, with particular emphasis to transformations ruled by diffusional growth which cannot be described by the Kolmogorov-Johnson-Mehl-Avrami (KJMA) theory. In order to bridge the gap between these two methods, the conditional probability functions entering the "Differential-Critical-Region" approach are determined in terms of correlation functions. The formulation of these probabilities by means of cluster expansion is also derived, which improves the accuracy of the computation. The model is applied to 2D and 3D parabolic growths occurring at constant value of either actual or phantom-included nucleation rates. Computer simulations have been employed for corroborating the theoretical modeling. The contribution to the kinetics of phantom overgrowth is estimated and it is found to be of a few percent in the case of constant value of the actual nucleation rate. It is shown that for a parabolic growth law both approaches do not provide a closed-form solution of the kinetics. In this respect, the two methods are equivalent and the longstanding overgrowth phenomenon, which limits the KJMA theory, does not admit an exact analytical solution.

DOI: 10.1103/PhysRevE.90.052406 PACS number(s): 81.15.Aa, 68.55.A−, 05.70.Fh

I. INTRODUCTION

In order to describe the kinetics of first-order phase transformations proceeding via nucleation and growth, researchers often make use of the Kolmogorov-Johnson-Mehl-Avrami (KJMA) approach which is based on Poisson statistics (no correlation among nuclei is present) [1–3]. The model has been extensively employed to tackle interesting problems in chemistry, electrochemistry, materials science, and biology, just to mention a few [4–12]. Investigation of the possibility to apply the KJMA theory to describe real systems has been the main purpose of several works that analyzed the effects on the kinetics of anisotropic growth [13–17], non-random nucleation [18,19], nucleus growth in the presence of defects [20], and nucleation and growth in different metrics [21].

The celebrated KJMA formula can be obtained through three methods, namely: i) the Kolmogorov method, which exploits Poisson statistics to find the probability that no nucleation event takes place in a given region of space [1]; ii) the Avrami approach which is based on set theory [3]; and iii) the differential-critical-region method introduced by Alekseechkin [22]. Moreover, we have combined approaches i) and ii) in [23] and have found the connection between Avrami's expansion in terms of extended volumes and the correlation functions in Ref. [24]. For the sake of clarity, it is worth recalling the difference between actual and phantom-included nucleation rates. The two nucleations distinguish between real nuclei (actual nucleation) and nuclei which can appear both in the untransformed and transformed phases. It goes without saying that the phantom-included nucleation process has simply a mathematical significance which, in turn, is limited to the Poisson process [25]. Accordingly, both Avrami and Kolmogorov methods make use of the phantom-included nucleation rate. Nonetheless, the mathematical description of the KJMA process can be likewise formulated in terms of the actual nucleation rate, while making use of correlation functions [19]. The correlation function approach (i.e., when employed with the actual nucleation rate) naturally resolves the question of phantom overgrowth, which limits the applicability of the KJMA model to a sub-set of growth laws. The differential-critical-region method [22] has also been improved to overtake the limit on the growth laws. The diffusional parabolic growth is a paradigmatic example of a growth law which the KJMA theory cannot describe [25–27]. In this respect both the differential-critical-region and the correlation-function-based approaches are suitable for treating phase transformations independently of the growth law. The time is ripe for a comparative critical analysis of these methods, aimed at highlighting not only their advantages and disadvantages but, above all, the connection between the physical quantities introduced in the two approaches. The very purpose of the present work is to perform such a comparison, as anticipated in our previous paper [28]. Notably, a general theory linking the physical quantities entering the two approaches will be developed and an explicit calculation up to second order terms will be discussed. Such a calculation exposes some limitations of the differential critical region method.

The paper is organized as follows. The first section is devoted to the differential-critical-region method and to the definition of appropriate probability functions that will be employed in the theory. In the second section, which is the core of the article, we evaluate the functional form of the above-mentioned probabilities in terms of correlation functions. The third section is devoted to the differential equation which is satisfied by these probabilities and the possibility of obtaining

*tomellini@uniroma2.it

their expressions in closed form. The last two sections are devoted to an application of the theory to diffusional growth and to comparison with computer simulations.

II. THEORY

A. Probability functions entering the differential-critical-region method

In the following we consider a random distribution of circular or spherical nuclei (2D and 3D phase transformations, respectively). Their growth law is given by the function $r(t_1,t)$ which is the radius, at time t, of the nucleus born at time t_1. The differential-critical-region method is based on a sort of kinetic equation for the probability that a point in space, chosen at random, is transformed in an infinitesimal interval of time dt. In the following, two nucleation rates will be considered, namely: i) the "phantom included" nucleation rate, $I_0(t)$, i.e., the nucleation takes place throughout the entire space independently of whether the nucleation point has been already transformed or not [3]; ii) the "actual" nucleation rate, $I_a(t)$, for which the nucleation in the untransformed phase is only considered. The relationship between the two nucleation rates reads $I_a(t) = I_0(t)[1-\xi(t)]$, where $0 < \xi(t) < 1$ is the fraction of transformed surface or the probability that a point in space, taken at random, is transformed at t. Let us consider a generic point, **c**, in space. Two events have to be defined, they are: i) A_t and ii) B_{t_1}. A_t is the event according to which the point **c** is untransformed at time t, B_{t_1} is the event according to which an actual nucleus is formed at t_1 (within dt_1) at distance $\mathbf{r} = r(t_1,t)\hat{\mathbf{r}}$ from **c** within $rd_trd\theta$ ($r^2d_trd\Omega$) with $d_tr = \partial_t r(t_1,t)dt$ and θ (Ω) being the 2D polar (3D solid) angle. To determine the kinetics the following differential probability has to be computed:

$$\begin{aligned} P(A_t \cap B_{t_1}) &= P(A_t|B_{t_1})P(B_{t_1}) \\ &= P(A_t)P(B_{t_1}|A_t), \end{aligned} \tag{1}$$

where $P(C|D)$ denotes the usual conditional probability that the C event occurs provided that the D event has occurred.

In other words, Eq. (1) is the probability that a generic point, **c**, is transformed between time t and $t+dt$ by an actual nucleus which starts growing between t_1 and t_1+dt_1 and located from **c** at distance **r** with $r = r(t_1,t)$ (Fig. 1). Let us now "translate" Eq. (1) to a more "physical" language more suitable for analytical computation. For the sake of simplicity, in the following the computation is presented for the 2D case. Nevertheless, the extension to the 3D case is straightforward as we will point out throughout the paper.

Let $d\xi(t_1,t) \equiv P(A_t|B_{t_1})P(B_{t_1})$ be rewritten as

$$d\xi(t_1,t) = P_c(t|t_1,\mathbf{r})d\tilde{P}_a(t_1,\mathbf{r}), \tag{2}$$

where $d\tilde{P}_a(t_1,\mathbf{r}) \equiv P(B_{t_1})$ and $P_c(t|t_1,\mathbf{r})$ is the conditional probability that the point **c** is untransformed at time t provided that the nucleation of an actual nucleus occurred at $(\mathbf{r},t_1)$. It turns out that

$$d\tilde{P}_a(t_1,\mathbf{r}) = I_a(t_1)r(t_1,t)d_trd\theta dt_1. \tag{3}$$

The last term of Eq. (1), $d\xi \equiv P(A_t)P(B_{t_1}|A_t)$, can be written according to

$$d\xi(t_1,t) = (1-\xi(t))dP_a(\mathbf{r},t_1|t), \tag{4}$$

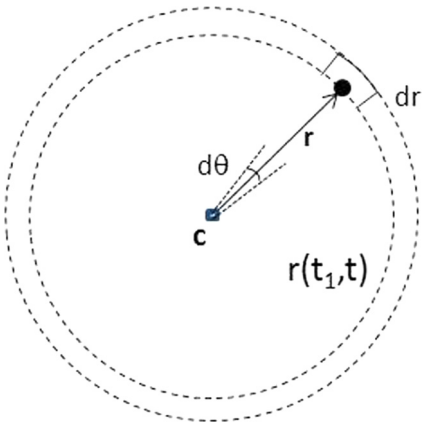

FIG. 1. (Color online) Sketch of the differential critical region ($d\mathbf{r} = rdrd\theta$) for the point **c** for 2D phase transformations. The nucleus which nucleates within $d\mathbf{r} = r(t_1,t)\partial_t r(t_1,t)dtd\theta$ at distance $r = r(t_1,t)\hat{\mathbf{r}}$ from **c** and in the time interval dt_1 at t_1, will transform **c** at t within dt.

where $1-\xi(t) \equiv P(A_t)$, and $dP_a(\mathbf{r},t_1|t)$ is the conditional probability that an actual nucleus nucleates at $(\mathbf{r},t_1)$ provided that the point **c** is untransformed until t. The last requirement guarantees that the point **c** is not transformed by an overgrowth phenomenon even if the nature of growth law allowed the overgrowth. The conditional probability reads

$$dP_a(\mathbf{r},t_1|t) = q(\mathbf{r},t_1|t)I_0(t_1)r(t_1,t)d_trd\theta dt_1, \tag{5}$$

where $q(\mathbf{r},t_1|t)$ is the conditional probability that the nucleation point (at relative distance $\mathbf{r} = r(t_1,t)\hat{\mathbf{r}}$ from **c**, within $rd_trd\theta$) is not transformed until t_1. As the system under analysis is homogeneous and isotropic, $P_c(t|t_1,\mathbf{r}) = P_c[t|t_1,r(t_1,t)]$ which will be denoted as $P_c(t|t_1)$ and, similarly, $q[r(t_1,t),t_1|t] \equiv q(t_1|t)$. Equations (2)–(5) imply

$$\begin{aligned} \frac{d\xi}{dt} &= 2\pi[1-\xi(t)]\int_0^t q(t_1|t)I_0(t_1)r(t_1,t)\partial_t r(t_1,t)dt_1 \\ &= 2\pi\int_0^t P_c(t|t_1)I_a(t_1)r(t_1,t)\partial_t r(t_1,t)dt_1, \end{aligned} \tag{6}$$

or, using the relationship between I_0 and I_a,

$$P_c(t|t_1) = q(t_1|t)\frac{1-\xi(t)}{1-\xi(t_1)}. \tag{7}$$

Equation (7) holds independently of the space dimension. Since in the KJMA model phantom overgrowth is precluded, $q(t_1|t) = 1$, so $P_c(t|t_1) = \frac{1-\xi(t)}{1-\xi(t_1)}$, namely the ratio between the (unconditional) probabilities that the generic point is untransformed at t and at $t_1 < t$. This probability is independent of the nucleation event occurring between t_1 and t_1+dt_1 at $r(t_1,t)\hat{\mathbf{r}}$. It is worth noting, in passing, that this probability function has been employed by Avrami to demonstrate the KJMA formula, in the form $\frac{1-\xi(t)}{1-\xi(t_1)} = \frac{v'(t_1,t)}{v_e(t_1,t)}$, where v' and v_e refer to the nonoverlapped and extended volumes of the nucleus, respectively [3,23].

We briefly comment on Eqs. (3) and (5), in the case of KJMA compliant growths. In fact, setting I_0 in place of I_a in Eq. (3), this equation coincides with Eq. (5) since, in this case, $q = 1$. However, the considered nucleation event is now

different for it includes any nucleus whether it is actual or phantom. As a consequence, $P(A_t|B_{t_1}) \to P(A_t) \equiv 1-\xi(t)$.

Although in the present paper the application will be presented for the Poissonian nucleation, the differential-critical-region method is much more versatile since, in principle, it can be employed for treating: i) Poissonian nucleation with growth laws which embody phantom overgrowth; ii) correlated nucleation with any kind of growth law. Nevertheless, from the theoretical perspective a significant open question is whether the integral form of the kinetics given by Eq. (6), also expressed as

$$1-\xi(t) = \exp\left[-\frac{D\pi^{D/2}}{\Gamma(D/2+1)}\int_0^t dt' \int_0^{t'} dt_1 q(t_1|t') I_0(t_1) \times r^{D-1}(t_1,t')\partial_{t'} r(t_1,t') dt_1\right], \tag{8}$$

admits a closed-form solution or not [29]. In Eq. (8) D is the space dimension and $\Gamma(x)$ the gamma function. Furthermore, in the case $q(t_1|t')=1$ the KJMA formula is easily obtained from Eq. (8) by exchanging the order of integration. From now on the cases $D=2,3$ will be considered.

B. Correlation-function-based approach

In previous works [30,31] we developed an approach based on correlation functions for describing phase transformation kinetics. In the following, we report the main formulas which are necessary to face the problem under examination. In particular, the fraction of untransformed phase is given in terms of f_n-functions through the expansion [30]

$$1-\xi(t) = 1 - \int_0^t dt_1 I(t_1) \int_{\Delta_{1t}} d\mathbf{r}_1 f_1(\mathbf{r}_1) + \int_0^t dt_1 I(t_1) \times \int_0^{t_1} dt_2 I(t_2) \int_{\Delta_{1t}} d\mathbf{r}_1 \int_{\Delta_{2t}} d\mathbf{r}_2 f_2(\mathbf{r}_1,\mathbf{r}_2) - \cdots \tag{9}$$

that can be rewritten as

$$1-\xi(t) = 1 + \sum_{m=1}^{\infty} \frac{(-)^m}{m!} \int_0^t dt_1 I(t_1) \cdots \int_0^t dt_m I(t_m) \times \int_{\Delta_{1t}} d\mathbf{r}_1 \cdots \int_{\Delta_{mt}} d\mathbf{r}_m f_m(\mathbf{r}_1,\mathbf{r}_2,\ldots,\mathbf{r}_m) \equiv 1 + \sum_{m=1}^{\infty} (-)^m \Im_m(t), \tag{10}$$

where $\Delta_{it} \equiv \Delta(t_i,t)$, $i=1,2,\ldots,m$, is the domain (a disk or a sphere in the present work) transformed at time t by a nucleus born at t_i. In Eqs. (9), (10) $[I(t_1)dt_1 d\mathbf{r}_1][I(t_2)dt_2 d\mathbf{r}_2]\cdots[I(t_m)dt_m d\mathbf{r}_m] f_m(\mathbf{r}_1,\ldots,\mathbf{r}_m)$ is the probability of finding nuclei born between t_i and t_i+dt_i in the volume elements $d\mathbf{r}_i$ around $\mathbf{r}_i$, irrespective of the position of the other $N-m$ nuclei, being N the total number of nuclei at t. For example, the $f_2(\mathbf{r}_i,\mathbf{r}_j)$ function is the well-known "radial distribution function" for the pair of nuclei (i,j). Moreover, Eq. (10) holds provided the f_m function is symmetric under the exchange of nucleus coordinates. For homogeneous systems $f_1(\mathbf{r}_1)=1$.

By introducing the function

$$F_m(t_1,\ldots,t_m;t) = \int_{\Delta_{1t}} d\mathbf{r}_1 \cdots \int_{\Delta_{mt}} d\mathbf{r}_m f_m(\mathbf{r}_1,\ldots,\mathbf{r}_m), \tag{11}$$

$\Im_m(t)$ becomes

$$\Im_m(t) = \frac{1}{m!}\int_0^t dt_1 I(t_1) \cdots \int_0^t dt_m I(t_m) F_m(t_1,\ldots,t_m;t). \tag{12}$$

The nucleation rate, $I(t)$, has to be defined in terms of the stochastic process under study. For example, in the case of KJMA compliant growths and unconditional (random) nucleation throughout the entire space, $I=I_0$, $f_n=(f_1)^n=1$ and Eq. (10) directly leads to the KJMA expression: $\xi(t) = 1-\exp[-\hat{X}_e(t)]$, with the phantom included extended surface $\hat{X}_e(t) = \int_0^t I_0(t')|\Delta(t',t)|dt'$, $|\Delta|$ being the measure of Δ. On the other hand, working with $I=I_a$ in Eqs. (9) and (10) entails correlation among nuclei being f_m's, in principle, different from zero. The use of the actual nucleation rate therefore allows one to deal with non-KJMA compliant growths in a rigorous fashion, at the cost of a more involved mathematical formulation [28].

Incidentally, the KJMA kinetics can be formulated in terms of actual nucleation. This has been done in Ref. [28] where, to simplify the mathematical computation, a constant value for the actual nucleation rate, I_a, and the time dependent phantom-included nucleation rate, $I_0(t) = \frac{I_a}{1-\xi(t)}$, have been considered.

Equation (10) can be rewritten in terms of correlation functions, g_m, according to

$$1-\xi(t) = \exp\left[\sum_{m=1}^{\infty} \frac{(-)^m}{m!} \int_0^t dt_1 I(t_1) \int_0^t dt_2 I(t_2) \cdots \times \int_0^t dt_m I(t_m) \int_{\Delta_{1t}} d\mathbf{r}_1 \int_{\Delta_{2t}} d\mathbf{r}_2 \cdots \times \int_{\Delta_{mt}} d\mathbf{r}_m g_m(\mathbf{r}_1,\mathbf{r}_2,\ldots,\mathbf{r}_m)\right], \tag{13}$$

where the g_m are linked to the f_m-functions by cluster expansion. Specifically, the first three functions read

$$\begin{aligned} f_1(\mathbf{r}_1) &= g_1(\mathbf{r}_1), \\ f_2(\mathbf{r}_1,\mathbf{r}_2) &= g_1(\mathbf{r}_1)g_1(\mathbf{r}_2) + g_2(\mathbf{r}_1,\mathbf{r}_2), \quad \text{and} \\ f_3(\mathbf{r}_1,\mathbf{r}_2,\mathbf{r}_3) &= g_1(\mathbf{r}_1)g_1(\mathbf{r}_2)g_1(\mathbf{r}_3) + g_2(\mathbf{r}_1,\mathbf{r}_2)g_1(\mathbf{r}_3) \\ &\quad + g_2(\mathbf{r}_1,\mathbf{r}_3)g_1(\mathbf{r}_2) + g_2(\mathbf{r}_2,\mathbf{r}_3)g_1(\mathbf{r}_1) \\ &\quad + g_3(\mathbf{r}_1,\mathbf{r}_2,\mathbf{r}_3). \end{aligned} \tag{14}$$

Since the f_m's are symmetric under the exchange of nucleus coordinates, Eq. (14) implies the g_m functions to share the same symmetry. Under these circumstances the following representation can be adopted for the argument of the exponential

in Eq. (13):

$$1-\xi(t)=\exp\left[\sum_{m=1}^{\infty}(-)^m\int_0^t dt_1 I(t_1)\int_0^{t_1}dt_2 I(t_2)\cdots \times\int_0^{t_{m-1}}dt_m I(t_m)\int_{\Delta_{1t}}d\mathbf{r}_1\int_{\Delta_{2t}}d\mathbf{r}_2\cdots \times\int_{\Delta_{mt}}d\mathbf{r}_m g_m(\mathbf{r}_1,\mathbf{r}_2,\ldots,\mathbf{r}_m)\right]. \quad (15)$$

The meaning of the $I(t)$ function entering Eqs. (13), (15) is also subject to the considered stochastic process, namely, to the functional form of the g_m's. In fact, KJMA compliant growths with $I=I_0$ imply $g_{m\geqslant 2}=0$ for, in this case, nuclei are randomly distributed throughout the whole space. For $g_{m\geqslant 2}=0$ Eq. (13) directly leads to the KJMA formula. On the other hand, if $I=I_a$, Eq. (13) entails correlation among nuclei with all the g_m's, in principle, different from zero.

C. Determination of $P_c(t|t_1)$ and $q(t_1|t)$ probabilities

In the following the general form $f_m(\mathbf{r}_1,\mathbf{r}_2,\ldots,\mathbf{r}_m,t_1,t_2,\ldots,t_m)\in C^1$ will be considered for the f_m-functions. Let us clarify a mathematical aspect which is important for computing the probabilities $P_c(t|t_1)$ and $q(t_1|t)$. This aspect is illustrated by considering the contribution of the f_2 term in Eqs. (9), (10). With reference to this term, we note that the integral over the spatial coordinates is symmetric in t_1,t_2. We denote this function as $F_2(t_1,t_2;t)$ (positive definite), where $F_2(t,t_2;t)=F_2(t_1,t;t)=0$. The last term in Eq. (9) becomes

$$\begin{aligned}\Im_2(t)&=\int_0^t dt_1 I(t_1)\int_0^{t_1}dt_2 I(t_2)F_2(t_1,t_2;t)\\&=\frac{1}{2}\int_0^t dt_1 I(t_1)\int_0^t dt_2 I(t_2)F_2(t_1,t_2;t),\end{aligned} \quad (16)$$

where in the last equality the symmetry of the function was exploited. The time derivative of $\Im_2$ [Eq. (16)] therefore implies

$$\begin{aligned}\dot{\Im}_2&=\frac{1}{2}\int_0^t dt_1 I(t_1)\int_0^t dt_2 I(t_2)\partial_t F_2(t_1,t_2;t)\\&\equiv\int_0^t dt_1 I(t_1)\int_0^{t_1}dt_2 I(t_2)\partial_t F_2(t_1,t_2;t).\end{aligned} \quad (17)$$

In other words, $\dot{\Im}_2$ has been expressed in the form $\dot{\Im}_2=\int_0^t dt_1 I(t_1)G(t_1,t)$. What is important to note is that, in general, $G(t_1,t)$ depends upon the representation of the double integral in Eq. (16). In fact, $G_a(t_1,t)=\frac{1}{2}\int_0^t dt_2 I(t_2)\partial_t F_2(t_1,t_2;t)$ and $G_b(t_1,t)=\int_0^{t_1}dt_2 I(t_2)\partial_t F_2(t_1,t_2;t)$ are not equal, given that $\partial_t F_2(t_1,t_2;t)|_{t_1=0}$ is, in general, different from zero [i.e., $G_a(0,t)\neq G_b(0,t)=0$].

In order to compare the two approaches we employ the following procedure: on the ground of the representation of ξ in terms of f_n functions [Eqs. (9), (10), (13), (15)] we determine the differential of the fractional coverage which should take the same form as Eq. (6), for both methods are assumed to be exact. Such a comparison allows one to compute, eventually, the $P_c(t|t_1)$ and $q(t_1|t)$ probabilities in terms of f_n and g_n functions. It is worth reminding that the probability functions satisfy the following constraints [Eq. (7)]: $q(0|t)=1$, $P_c(t|0)=1-\xi(t)$. These conditions are important since they suggest a convenient representation of the ξ probability for computing its differential.

As far as the evaluation of P_c is concerned, the representation of ξ grounded on Eq. (10) is employed. One observes that the derivative of Eq. (12) only requires the derivative of the F_m function. Exploiting polar coordinates and the condition $F_m(t_1,\ldots,t_m;t)|_{t_k=t}=0,\forall k\in[1,..,m]$ one gets (2D case)

$$\begin{aligned}\dot{\Im}_m(t)=&\frac{m}{m!}\int_0^t dt_1 I(t_1)R_{1t}\partial_t R_{1t}\int_0^t dt_2 I(t_2)\cdots\\&\times\int_0^t dt_m I(t_m)\int d\theta_1\int_{\Delta_{2t}}d\mathbf{r}_2\cdots\\&\times\int_{\Delta_{mt}}d\mathbf{r}_m f_m(\mathbf{r}_1,\ldots,\mathbf{r}_m,t_1,\ldots,t_m)|_{\mathbf{r}_1=R_{1t}\hat{\mathbf{r}}_1},\end{aligned} \quad (18)$$

where $r(t_1,t)=R(t_1,t)\equiv R_{1t}$. Comparing the expression $\dot{\xi}(t)=\sum_{m=1}^{\infty}(-)^{m-1}\dot{\Im}_m(t)$, where $I(t)=I_a(t)$ with Eq. (6), we obtain for isotropic system, eventually,

$$\begin{aligned}P_c(t|t_1)=&1+\sum_{m=2}^{\infty}\frac{(-)^{m-1}}{(m-1)!}\int_0^t dt_2 I_a(t_2)\cdots\\&\times\int_0^t dt_m I_a(t_m)\int_{\Delta_{2t}}d\mathbf{r}_2\cdots\\&\times\int_{\Delta_{mt}}d\mathbf{r}_m f_m(\mathbf{r}_1,\ldots,\mathbf{r}_m,t_1,\ldots,t_m)|_{\mathbf{r}_1=R_{1t}\hat{\mathbf{r}}_1},\end{aligned} \quad (19)$$

which holds for any space dimension.

As noted in Sec. II A for KJMA growths, if in Eq. (19) I_a is substituted by I_0 one obtains, as expected, $P(A_t)\equiv\sum_{m=0}^{\infty}\frac{(-)^m}{m!}\hat{X}_e(t)^m=1-\xi(t)$. Moreover, for a homogeneous system the cluster expansion technique makes it possible to express the P_c probability as (see also the Appendix A for details)

$$\begin{aligned}P_c(t|t_1)=\exp&\left[\sum_{m=1}^{\infty}\frac{(-)^m}{m!}\int_0^t d\tau_1 I_a(\tau_1)\cdots\right.\\&\times\int_0^t d\tau_m I_a(\tau_m)\int_{\Delta_{1t}}d\mathbf{x}_1\cdots\\&\left.\times\int_{\Delta_{mt}}d\mathbf{x}_m\tilde{g}_m(\mathbf{x}_1,\ldots,\mathbf{x}_m,t_1,\tau_1,\ldots,\tau_m)\right]\end{aligned} \quad (20)$$

with $\Delta_{it}\equiv\Delta(\tau_i,t)$ and $\mathbf{x}_i=\mathbf{r}_{i+1}-R(t,t_1)\hat{\mathbf{r}}_1$ the relative coordinate. The functions $\tilde{g}_m$ are defined by the following cluster expansion:

$$\begin{aligned}\bar{f}_1(1)&=\tilde{g}_1(1),\\\bar{f}_2(1,2)&=\tilde{g}_1(1)\tilde{g}_1(2)+\tilde{g}_2(1,2),\\\bar{f}_3(1,2,3)&=\tilde{g}_1(1)\tilde{g}_1(2)\tilde{g}_1(3)+\tilde{g}_2(1,2)\tilde{g}_1(3)\\&\quad+\tilde{g}_2(1,3)\tilde{g}_1(2),+\tilde{g}_2(2,3)\tilde{g}_1(1)+\tilde{g}_3(1,2,3),\end{aligned} \quad (21)$$

and so on, where $\bar{f}_{m-1}(\mathbf{x}_1,\ldots,\mathbf{x}_{m-1},t_1,\tau_1,\ldots,\tau_{m-1})\equiv f_m(\mathbf{x}_1,\ldots,\mathbf{x}_{m-1},t_1,\tau_1,\ldots,\tau_{m-1})$.

The computation of $q(t_1|t)$ is based on the representation of ξ in terms of g_m correlation functions, Eq. (15), where the exponential form ensures that its derivative provides the multiplicative factor $[1-\xi(t)]$ of Eq. (6). Following a similar computation pathway as above, the derivative of Eq. (15) is (2D case)

$$\frac{d\xi}{dt} = [1-\xi(t)]2\pi \int_0^t dt_1 I_0(t_1)[1-\xi(t_1)]R_{1t}\partial_t R_{1t}\left[1+\frac{1}{2\pi}\sum_{m=2}^{\infty}(-)^{m-1}\int d\theta_{i_m}\int_0^{t_1} dt_2 I_a(t_2)\cdots\int_0^{t_{m-1}} dt_m I_a(t_m)\right.$$
$$\left.\times\sum_{i_m=1}^{m}\frac{R_{i_m t}\partial_t R_{i_m t}}{R_{1t}\partial_t R_{1t}}\int_{\Delta_{i_1 t}} d\mathbf{r}_{i_1}\cdots\int_{\Delta_{i_{m-1}t}} d\mathbf{r}_{i_{m-1}} g_m(\mathbf{r}_{i_1},\ldots,\mathbf{r}_{i_m},t_{i_1},\ldots,t_{i_m})|_{\mathbf{r}_{i_m}=R_{i_m t}\hat{\mathbf{r}}_{i_m}}\right], \tag{22}$$

where in the sum the i_k's take the values $1,2,\ldots,m$ with $i_1\neq i_2\neq\ldots\neq i_m$ and the expression $I_a(t)=I_0(t)[1-\xi(t)]$ has been used in the first integral. In the case of power growth laws no singularity is expected at $t=t_1$ for $\frac{1}{R(t-t_1)\partial_t R(t-t_1)}\int_{\Delta_{1t}} d\mathbf{r}_1 \sim (t-t_1)$. Comparison with Eq. (6) leads to

$$q(t_1|t) = [1-\xi(t_1)]\left[1+\frac{1}{2\pi}\sum_{m=2}^{\infty}(-)^{m-1}\int d\theta_{i_m}\int_0^{t_1} dt_2 I_a(t_2)\cdots\int_0^{t_{m-1}} dt_m I_a(t_m)\sum_{i_m=1}^{m}\frac{R_{i_m t}\partial_t R_{i_m t}}{R_{1t}\partial_t R_{1t}}\int_{\Delta_{i_1 t}} d\mathbf{r}_{i_1}\cdots\right.$$
$$\left.\times\int_{\Delta_{i_{m-1}t}} d\mathbf{r}_{i_{m-1}} g_m(\mathbf{r}_{i_1},\ldots,\mathbf{r}_{i_m},t_{i_1},\ldots,t_{i_m})|_{\mathbf{r}_{i_m}=R_{i_m t}\hat{\mathbf{r}}_{i_m}}\right]. \tag{23}$$

Equation (23) can be generalized to the 3D case provided $R_{i_k t}^2\partial_t R_{i_k t}$, $d\Omega_{i_k}$, and 4π are used in place of $R_{i_k t}\partial_t R_{i_k t}$, $d\theta_{i_k}$, and 2π, respectively. Equation (23) satisfies the required limit $q(0|t)=1$. Notably, in Eq. (23) the multiplicative factor, $[1-\xi(t_1)]$, is the (unconditional) probability the nucleation takes place in the uncovered portion of the surface.

D. Differential equation for $q(t_1|t)$

Until now the functions $P_c(t|t_1)$ and $q(t_1|t)$ have been expressed by using the correlation function approach; in particular, in Appendix A $P_c(t|t_1)$ has been explicitly computed retaining the lowest-order term $\tilde{g}_1$ in the argument of the exponential. The fact that $\xi(t)$ is not given in closed form (apart from the KJMA case) rules out the ambitious goal to express $q(t_1|t)$ in closed form too, by means of a differential equation for $q(t_1|t)$. Starting from Eq. (23), i.e., $q(t_1|t)=[1-\xi(t_1)]S(t_1,t)$, one obtains

$$\partial_{t_1} q = -\frac{d\xi}{dt_1}S(t_1,t)+[1-\xi(t_1)]\partial_{t_1}S$$
$$= -\frac{q(t_1|t)}{1-\xi(t_1)}\frac{d\xi}{dt_1}+q(t_1|t)\partial_{t_1}\ln S, \tag{24}$$

where the series $S(t_1,t)$ is defined through Eq. (23). By using Eq. (6), Eq. (24) can be rewritten as

$$\frac{\partial \ln q}{\partial t_1} = -\left[\int_0^{t_1} q(t_2|t_1)I_0(t_2)\frac{\partial|\Delta_{12}|}{\partial t_1}dt_2-\frac{\partial \ln S}{\partial t_1}\right], \tag{25}$$

where $|\Delta_{12}|=\frac{\pi^{D/2}}{\Gamma(D/2+1)}R_{12}^D$. Since $|\Delta_{12}|=\omega_D(R_{12},R_{2t};R_{1t})+\varpi_D(R_{12},R_{2t};R_{1t})$, $\varpi_D(R_{12},R_{2t};R_{1t})$ is the overlap area ($D=2$) or volume ($D=3$) between two nuclei of radius $R(t_2,t_1)=R_{12}$ and $R(t_2,t)=R_{2t}$ whose centers are $R(t_1,t)=R_{1t}$ apart (Fig. 2), Eq. (25) takes the form

$$\frac{\partial \ln q}{\partial t_1} = -\int_0^{t_1} q(t_2|t_1)I_0(t_2)\frac{\partial\omega_D(R_{12},R_{2t};R_{1t})}{\partial t_1}dt_2$$
$$-\left[\int_0^{t_1} q(t_2|t_1)I_0(t_2)\frac{\partial\varpi_D(R_{12},R_{2t};R_{1t})}{\partial t_1}dt_2-\frac{\partial \ln S}{\partial t_1}\right]. \tag{26}$$

Equation (26) can be traced back to the equation proposed by Alekseechkin in Ref. [27] provided the last term in the square brackets is negligible. In the next section this issue is further discussed in the ambit of the parabolic growth law.

The fact that the differential equation for $q(t_1|t)$ is not given in closed-form is also supported by the following demonstration based on the differential-critical-region method. Although the demonstration will be presented for the 2D case, it can be easily reformulated for any spatial dimension.

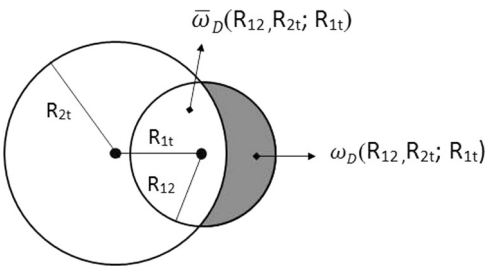

FIG. 2. Graphical representation of the $\omega_D(R_{12},R_{2t};R_{1t})$ and $\varpi_D(R_{12},R_{2t};R_{1t})$ quantities defined in the text. $\varpi_D(R_{12},R_{2t};R_{1t})$ is the overlap area (volume) between two nuclei of radii R_{2t} and R_{12} at relative distance R_{1t}. The quantities ω_D and ϖ_D sum up to $|\Delta_{12}|=\pi R_{12}^2$ (2D) and $|\Delta_{12}|=\frac{4\pi}{3}R_{12}^3$ (3D).

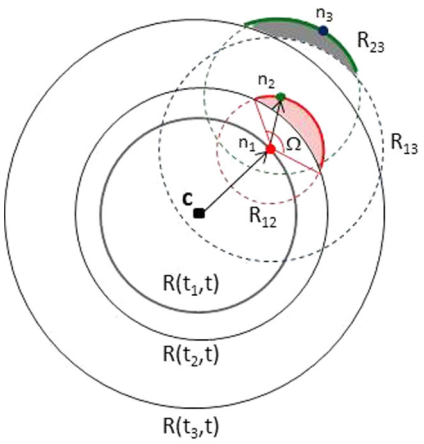

FIG. 3. (Color online) Pictorial view of the differential critical regions entering the definition of the conditional probability $q(t_1|t)$ discussed in Sec. II D. At time t, the critical region of **c** is the thick circular shell of radius $R(t_1,t)$ (circle in grey). The conditional probability $q(t_1|t)$ is equal to the fraction of the untransformed area of this shell at time t_1 ($t_1 < t$), given that the point **c** is untransformed up to t. In this shell the actual nucleus, n_1, will transform **c** at time t within dt. The "conditional" critical region for n_1 is also depicted as red thick line for a generic nucleus at distance $R(t_2,t_1) = R_{12}$ ($t_2 < t_1$). Owing to the requirement that **c** is untransformed at t, only a fraction of the circle centered at n_1 of radius R_{12} has to be considered, i.e., the portion protruding the circles $R(t_2,t)$ within the angle $\Omega = \Omega(t_2,t_1,t)$. The fraction of the untransformed area of this shell provides the higher order function $q^{(2)}(t_2|t_1,t)$ which enters Eq. (33). In a similar fashion one also defines the critical region for n_2 (green thick line) and the higher order probability $q^{(3)}(t_3|t_2,t_1,t)$ which is subjected to the condition that **c**, n_1 and n_2 are all untransformed until t, t_1, and t_2, respectively.

To begin with, we consider the definition of $dP_a(t_1|t)$ as the probability that an actual nucleation event (n_1 in Fig. 3) takes place in the shell of area $2\pi r(t_1,t)d_t r$ in the time interval dt_1 around t_1, given that the generic point **c** is untransformed until t [Fig. 3, thick circle of radius $R(t_1,t)$]. From Eq. (5) and considering for the sake of simplicity $I_0 = \text{const}$, we get

$$dP_a(t_1|t) = q(t_1|t)[I_0 2\pi r(t_1,t)d_t r dt_1] = \delta N_a(t_1|t), \quad (27)$$

thus $\delta N_a(t_1|t)$ is the number of actual nuclei formed in the shell $2\pi r(t_1,t)d_t r$ within dt_1 given that the generic point **c** is untransformed until t. The term in the square brackets of Eq. (27) is the number of nucleation events, $\delta N(t_1,t)$, in the considered shell, therefore

$$q(t_1|t) = \frac{\delta N_a(t_1|t)}{\delta N(t_1,t)}. \quad (28)$$

Incidentally, the last equation can be reformulated as given in Ref. [27]

$$q(t_1|t) = \left(\frac{\delta A_a(t_1,t)}{\delta A(t_1,t)}\right)^{(1)}_{\Omega=2\pi} = X(t_1|t) = 1 - \xi(t_1|t), \quad (29)$$

where $X(t_1|t)$ is the fraction of the shell area δA that is untransformed at t_1 provided the point **c** is untransformed until t. In other words, $q(t_1|t)$ is the probability a point located at $r(t_1,t)$ from **c** is untransformed at t_1 given that the point **c** is untransformed at t. From Eqs. (29) and (4)–(6), one obtains

$$\begin{aligned} dq(t_1|t) &= -d\xi(t_1|t) \\ &= -q(t_1|t)\int_0^{t_1}\left(\frac{dP_a(t_2|t_1,t)}{dt_2}\right)dt_2. \end{aligned} \quad (30)$$

In Eq. (30) $dP_a(t_2|t_1,t)$ is the probability that an actual nucleus (n_2 in Fig. 3) is formed within the shell centered at n_1 of radius R_{12} and thickness $d_{t_1}r = \partial_{t_1} r(t_2,t_1)dt_1$ in the time interval dt_2 ($t_2 < t_1$), given the two conditions: i) **c** is untransformed until t; ii) n_1 is untransformed until $t_1 < t$. On the basis of the same argument that led to Eq. (27), one obtains

$$\begin{aligned} dP_a(t_2|t_1,t) &= q^{(2)}(t_2|t_1,t)[I_0\Omega(t_2,t_1,t)r(t_2,t_1)d_{t_1}r dt_2] \\ &= \delta N_a(t_2|t_1,t), \end{aligned} \quad (31)$$

where $\Omega(t_2,t_1,t)$ is the angle subtended by the nucleation zone for n_2 that is, in Fig. 3, the red thick arch of the circle of radius R_{12} centered at n_1. Consequently, $q^{(2)}(t_2|t_1,t) = (\frac{\delta A_a}{\delta A})^{(2)}_{\Omega(t_1,t_2,t)}$, which is the untransformed portion of the shell area subtended by $\Omega(t_2,t_1,t)$ (Fig. 3). The differential equation of $q(t_1|t)$ becomes

$$\begin{aligned} dq(t_1|t) = -q(t_1|t)dt_1 \int_0^{t_1} & q^{(2)}(\tau|t_1,t) \\ & \times [I_0\Omega(\tau,t_1,t)r(\tau,t_1)\partial_{t_1} r(\tau,t_1)d\tau], \end{aligned} \quad (32)$$

and, eventually [$q(0|t) = 1$]

$$\begin{aligned} q(t_1|t) = \exp\Bigg(-\int_0^{t_1} d\tau \int_0^{\tau} & d\tau' q^{(2)}(\tau'|\tau,t) I_0\Omega(\tau',\tau,t) \\ & \times r(\tau',\tau)\partial_\tau r(\tau',\tau)\Bigg). \end{aligned} \quad (33)$$

Equation (33) is not an integral equation for $q(t_1|t)$, since the functions $q(\tau'|\tau)$ and $q^{(2)}(\tau'|\tau,t)$ are different. In general, the higher-order (unknown) probability, $q^{(m)}(t_m|t_{m-1},\ldots,t_1,t)$, has to be introduced in order to estimate $q^{(m-1)}(t_{m-1}|t_{m-2},\ldots,t_1,t)$. As a consequence, the differential critical region method does not lead to a closed-form solution of the longstanding overgrowth problem, in similar fashion as the correlation-function-based approach discussed here. Nevertheless, in this context there exists a difference between the two methods. The correlation-function based approach gives the solution as a series which could be estimated, in principle, at the desired degree of approximation. On the other hand, in the framework of the differential-critical-region method the solution of the kinetics relies on the approximate closed-form of the differential equation Eq. (26) [27]. In turn, this last equation has been actually obtained by means of the correlation-function-based method.

Notably, in the case of growth laws that are consistent with the KJMA model, the angle $\Omega(\tau',\tau,t)$ vanishes and Eq. (33) implies $q(t_1|t) = 1$. In fact, from Fig. 3 it stems that $\Omega(t_2,t_1,t) \neq 0$ provided that $R_{1t} + R_{12} > R_{2t}$. For instance, such a condition is not satisfied by power laws with power exponents greater than or equal to unity (KJMA compliant growths).

III. APPLICATION TO PARABOLIC GROWTH

A. Kinetics of growth

The growth law is defined as $R(t',t) = v\sqrt{t-t'}$ and implies the phantom overgrowth phenomenon. In the framework of the correlation-function-based approach, in order to get rid of phantoms, i.e., of overgrowth, it is compulsory to formulate the theory in terms of the actual nucleation. For this purpose a hard-core-like model must be used. Moreover, since nucleation densities in real systems are usually small (of the order of 10^{-4} per site), approximate expressions for the f_m's can be employed. On the other hand, beyond these approximations the analytical computation does become prohibitive.

The lowest order terms of the f_m-functions are given by

$$\begin{aligned} f_2(\mathbf{r}_1,\mathbf{r}_2,t_1,t_2) &= H[|\mathbf{r}_{12}| - r(t_1,t_2)], \\ f_m(\mathbf{r}_1,\mathbf{r}_2,\ldots,\mathbf{r}_m,t_1,t_2,\ldots,t_m) &= \prod_{i<j} f_2(\mathbf{r}_i,\mathbf{r}_j,t_i,t_j), \end{aligned} \tag{34}$$

where $H(x)$ is the Heaviside function and $\mathbf{r}_{12} = \mathbf{r}_1 - \mathbf{r}_2$. In Eq. (34) the superposition principle has been employed which is expected to hold in the low-density limit [32]. The time dependence of the growth law is usually of the form $r(t',t) = r(t-t')$; consequently, in Eq. (34) the argument of the Heaviside function can be written as $f_2(\mathbf{r}_1,\mathbf{r}_2,t_1,t_2) = H[|\mathbf{r}_{12}| - r(|t_1-t_2|)]$ that is symmetric under the exchange of nucleus coordinates. In the following, we apply Eq. (20) by considering the contribution of the f_2-function. In this context a comment is in order. Strictly speaking, the equations derived above for P_c and q hold for f-functions belonging to the class C^1. Accordingly, care must be taken in applying the above formulation to the hard core model, owing to possible edge effects resulting from differentiation under the integral sign. However, it is shown that this effect is negligible on the kinetics of the transformation. The edge-effect on the P_c probability is discussed in the next section.

Inserting Eq. (34) into Eq. (20) and performing the integration over the $\mathbf{r}_2$ variable [see also Eqs. (A10), (A11) in Appendix A) one obtains a term containing the overlap area (volume) $\varpi_D(R_{12},R_{2t};R_{1t})$ (Fig. 2). The integration domain of the spatial integral is illustrated in Fig. 4 for parabolic growth at $t_2 > t_1$ and $t_1 > t_2$ (panels a, b). For the sake of completeness, the case of linear growth is also illustrated where, for $t_1 < t_2$, $\varpi_D = 0$ (panels c and d).

To simplify the complexity of the mathematical computation the case $I_a(t) = \text{const}$ is initially treated. Under these circumstances the general expression for $P_c(t|t_1)$ becomes

$$P_c(t|t_1) \cong \exp[-X_e(t)(1-b(\tau_1))] \quad , \tag{35}$$

where, $X_e(t) = \frac{\pi^{D/2}}{\Gamma(D/2+1)}\int_0^t I_a(t')R^D(t',t)dt'$ is the actual extended transformed fraction,

$$\begin{aligned} b(\tau_1) = {} & \frac{Dn+1}{\pi^{D/2}}\Gamma(D/2+1) \\ & \times \int_0^1 \varpi_D[(1-\tau_2)^n,(|\tau_1-\tau_2|)^n;(1-\tau_1)^n]d\tau_2 \end{aligned} \tag{36}$$

with $\tau_i = \frac{t_i}{t} \leqslant 1$ $(i = 1,2)$, $R(t',t) = v(t-t')^n$, and n being the growth exponent ($n = 1/2$ and $n = 1$ for parabolic and linear growths, respectively). On the basis of a scaling argument we also infer that the conditional probability scales as $-\ln P_c(t,\tau_1) = X_e(t) + \sum_{k=1}^{\infty} C_k(\tau_1)X_e(t)^k$, where the C_k functions are the coefficients of the expansion.

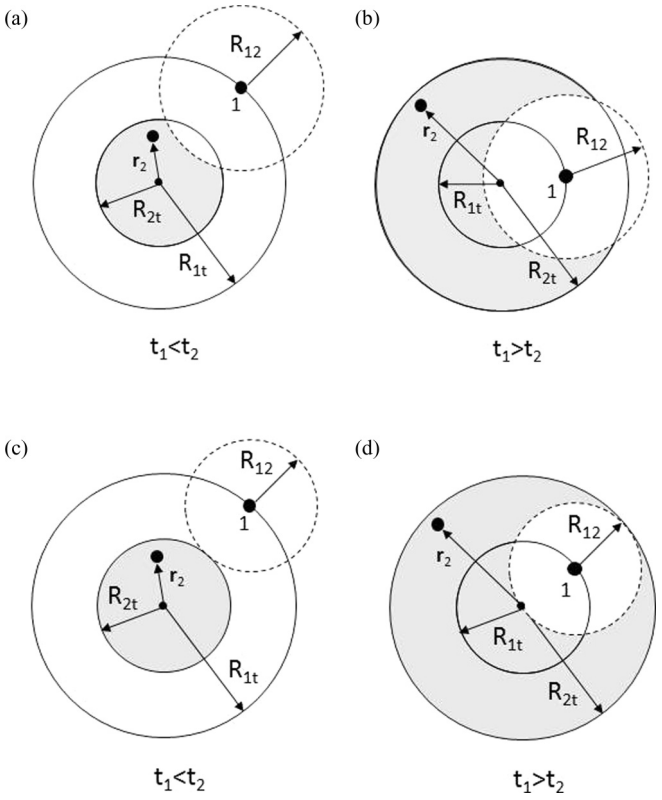

FIG. 4. Integration domains, R_{1t} and R_{2t}, employed for computing second-order terms of the $P_c(t|t_1)$ probability for both $t_1 > t_2$ and $t_1 < t_2$. (a), (b) and (c), (d) refer to the parabolic and linear growths, respectively. In the panels the circles of radius $R(t_2,t_1) = R_{12}$ are also displayed; they are linked to the hard core correlation employed to deal with actual nucleation. To compute Eq. (20) the position of nucleus 1 is fixed at R_{1t}. In the case of linear growth $\varpi_D(R_{12},R_{2t};R_{1t}) = 0$ for $t_1 < t_2$ (c).

For parabolic growth, the overlap area and volume read

$$\begin{aligned} & \varpi_2(R_{12},R_{2t};R_{1t}) \\ & = v^2(t-t_2)\arccos\frac{2t-t_2-t_1+|t_1-t_2|}{2\sqrt{(t-t_2)(t-t_1)}} \\ & \quad + v^2|t_1-t_2|\arccos\frac{t_2-t_1+|t_1-t_2|}{2\sqrt{|t_1-t_2|(t-t_1)}} \\ & \quad - \frac{1}{2}v^2\sqrt{4|t_1-t_2|(t-t_1)-(|t_1-t_2|+t_2-t_1)^2}, \end{aligned} \tag{37}$$

$$\begin{aligned} & \varpi_3(R_{12},R_{2t};R_{1t}) \\ & = \frac{2\pi}{3}v^3(|t_1-t_2|^{3/2}+(t-t_2)^{3/2}) + \frac{\pi}{12}v^3(t-t_1)^{3/2} \\ & \quad - \frac{\pi}{2}v^3(t-t_1)^{1/2}[t-t_2+|t_1-t_2|] \\ & \quad - \frac{\pi}{4}v^3\frac{[t-t_2-|t_1-t_2|]^2}{(t-t_1)^{1/2}} \end{aligned} \tag{38}$$

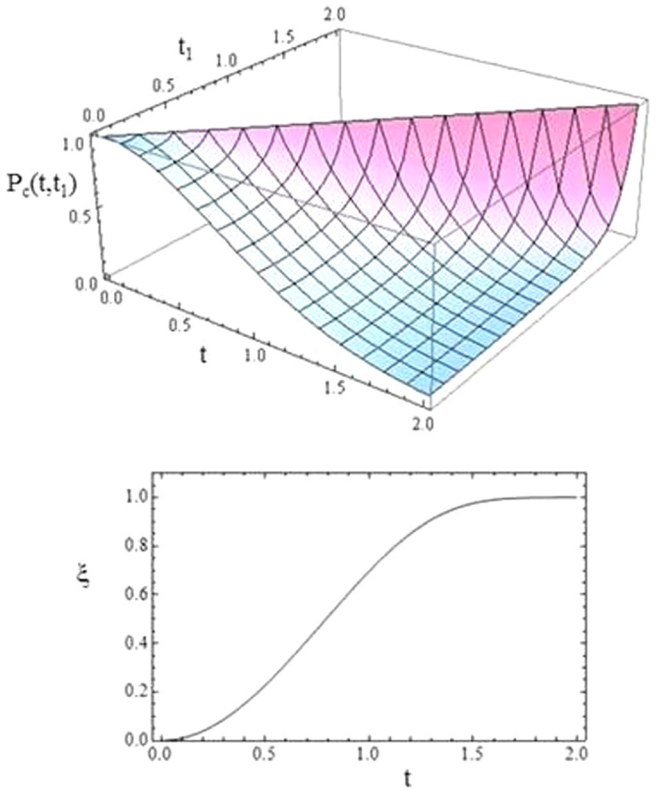

FIG. 5. (Color online) Behavior of the conditional probability $P_c(t|t_1)$ computed using Eq. (35) in the case of 2D parabolic growth, $n = 1/2$, and constant value of the actual nucleation rate I_a. The time variables, t and t_1, have been normalized to the quantity $(\pi I_a v^2/2)^{-1/2}$, i.e., $t = X_e^{1/2}$ and $t_1 = t\tau_1$ are dimensionless variables. In the lower panel it is reported the computer simulation of the kinetics of the surface coverage as a function of dimensionless time, t.

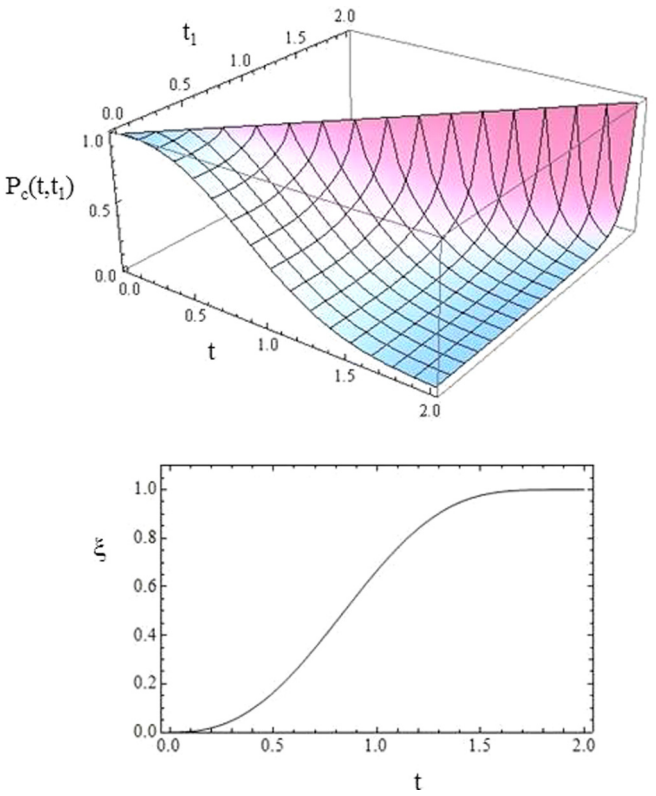

FIG. 6. (Color online) Behavior of the conditional probability $P_c(t|t_1)$ computed using Eq. (35) in the case of 3D parabolic growth, $n = 1/2$, and constant value of the actual nucleation rate I_a. The time variables, t and t_1, have been normalized to the quantity $(8\pi I_a v^3/15)^{-2/5}$, i.e., $t = X_e^{2/5}$ and $t_1 = t\tau_1$ are dimensionless variables. In the lower panel it is reported the computer simulation of the kinetics of the volume fraction as a function of dimensionless time, t.

with the extended area $X_e(t) = \frac{\pi}{2} I_a v^2 t^2$ and extended volume $X_e(t) = \frac{8\pi}{15} I_a v^3 t^{5/2}$. The $P_c(t|t_1)$ function, as computed from Eqs. (35)–(38), has been displayed in Figs. 5, 6 as a function of t and t_1. In particular, the time variable has been normalized to the quantity $(\pi I_a v^2/2)^{-1/2}$ and $(8\pi I_a v^3/15)^{-2/5}$, to get $X_e(t) = t^2$ (2D case) and $X_e(t) = t^{5/2}$ (3D case), respectively. Figures 5 and 6 also report the kinetics of the surface and volume fractions obtained through computer simulations at $I_a = \text{const}$. Specifically, simulations of 2D phase transitions by nucleation and growth have been performed on a square lattice whose dimension is $M \times M$. Simulations were performed for $M = 500, 1000$, and 2000 and at $I_a = \text{const}$ and no significant differences between the three sets of kinetics were detected. Also, the kinetics is found to depend only on the X_e variable in agreement with the analytical approach. The simulation also provides the phantom-included kinetics which differs from ξ owing to the overgrowth events. The computer outputs are plotted in Fig. 7(a) as a function of the extended actual surface, X_e, together with the kinetics for the linear growth (at constant I_a). The contribution of phantoms, $\Delta\xi$, highlighted in the inset of Fig. 7(a), entails a deviation of the KJMA formula from the actual kinetics that is lower than 0.02. This result is in agreement with previous studies on the contribution of phantoms performed for the nucleation rate $I_0 = \text{const}$ [26]. In order to check the reliability of the simulation, with respect to phantom overgrowth, we evaluated their contribution analytically. In fact, the effect of phantom overgrowth can be estimated by computing the extended surface (phantom included) entering the KJMA-equation: $\xi_{KJMA} = 1 - \exp[-\hat{X}_e(X_e)]$. It is possible to show that for parabolic growth

$$\hat{X}_e(X_e) = \int_0^{X_e} \frac{1}{1-\xi(y)} \left[\left(\frac{X_e}{y} \right)^{1/2} - 1 \right] dy, \qquad (39)$$

namely, a relationship between the phantom included extended surface and the transformed surface, $\xi(X_e)$. Using the $\xi(X_e)$ function obtained by the simulation, Eq. (39) implies a maximum value of $\Delta\xi$ equal to 0.0156 in comparison with 0.016 from Fig. 7(a).

As far as the 3D case is concerned, computer simulations have been performed on a square lattice $M \times M \times M$ at constant I_a and for $n = 1$ and $n = 1/2$ ($M = 200$). The computer simulations are shown in Fig. 7(b) as a function of the actual extended volume, X_e, for $n = 1/2$ (solid lines) and $n = 1$ (dashed line). Also, the contribution of phantoms, $\Delta\xi$, is highlighted in the inset of Fig. 7(b) and, as in the 2D case, the behavior of the KJMA formula slightly differs from the actual kinetics (about 0.01). The model can also be employed to compute the $P_c(t|t_1)$ and $q(t_1|t)$ functions in the case of linear

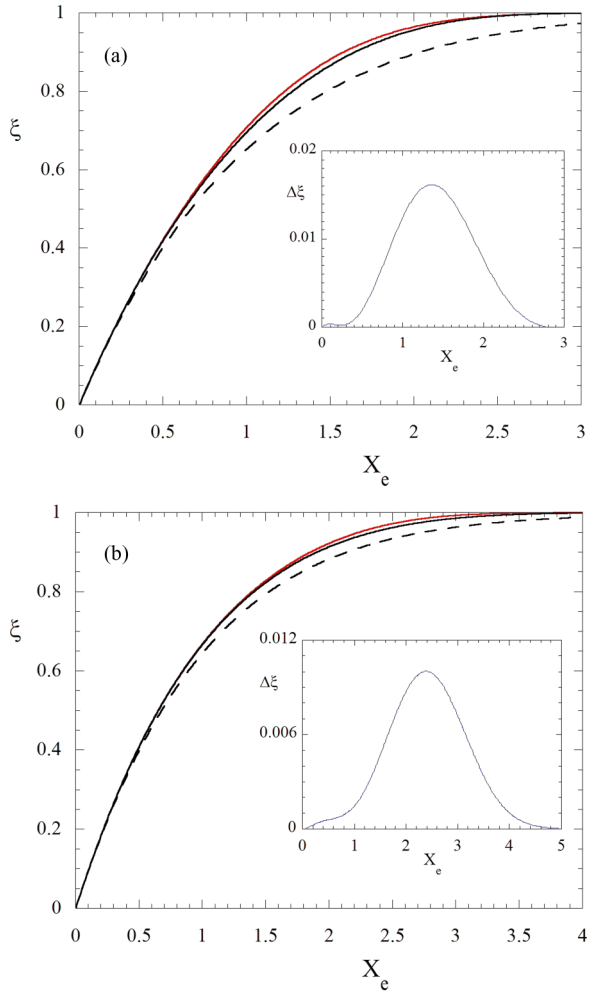

FIG. 7. (Color online) (a) Computer simulation of 2D phase transformations ruled by parabolic growth of circular nuclei for constant value of the actual nucleation rate, I_a, (black solid line). The computer simulation of the phantom-included kinetics (KJMA-kinetics ξ_{KJMA}), which implies phantom overgrowth, is reported as red solid line. The contribution of phantoms to the kinetics is displayed in the inset where $\Delta\xi = \xi_{KJMA} - \xi$. The kinetics for linear growth is also shown as dashed line. (b) The same as in (a) for the 3D case.

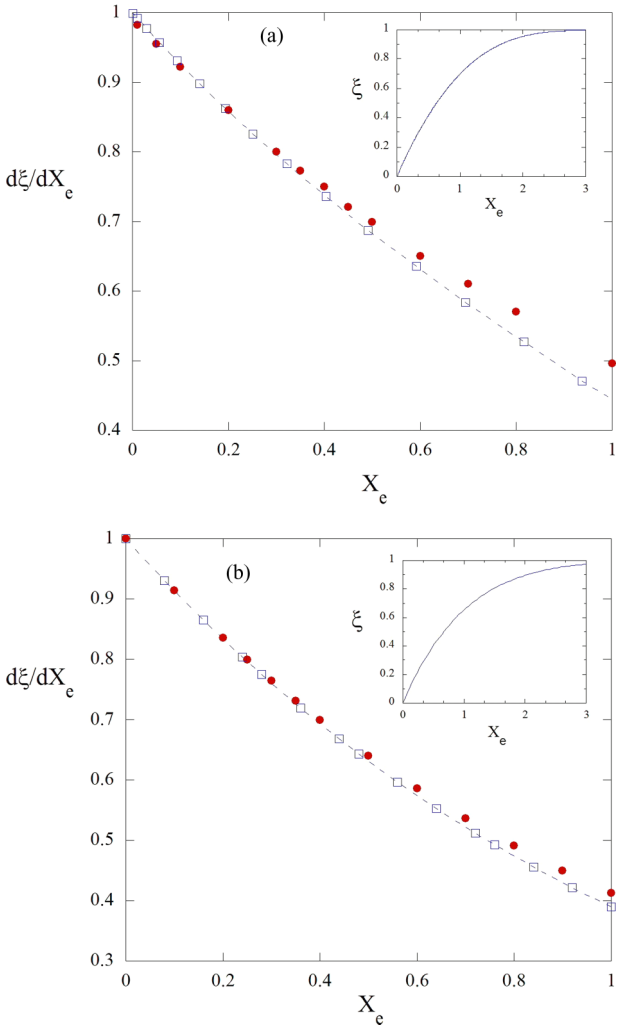

FIG. 8. (Color online) 2D phase transition. (a) Dimensionless rate $\frac{d\xi}{dX_e}$, computed using Eq. (41) and the $P_c(t|t_1)$ probability of Fig. 5, as a function of the extended surface for parabolic growth ($n = 1/2$) and constant value of the actual nucleation rate (solid symbols). The same quantity, as obtained by computer simulation, is also displayed (open symbols and dashed line). (b) Dimensionless rate $\frac{d\xi}{dX_e}$ for linear growth and constant value of the actual nucleation rate computed through Eq. (41) at $n = 1$ (solid symbols). The derivative of the KJMA kinetics is displayed as open symbols and dashed line. The kinetics of the surface fraction $\xi(X_e)$ vs actual extended surface, are reported in the insets.

growth where $q = 1$ is expected. The $P_c(t|t_1)$ function is given by Eq. (35) where, for $n = 1$, Eq. (36) provides $b(\tau_1) = \tau_1^{D+1}$. Since for linear growth $\frac{X_e(t_1)}{X_e(t)} = \tau_1^{D+1} \equiv b(\tau_1)$ we get

$$P_c(t|t_1) \cong \exp\{-[X_e(t) - X_e(t_1)]\}. \tag{40}$$

Moreover, at the same order of approximation as Eq. (40) the fraction of untransformed phase, Eq. (15), is equal to $1 - \xi \cong \exp[-X_e]$. Consequently, $P_c(t|t_1) \cong \frac{1-\xi(t)}{1-\xi(t_1)}$ which implies $q(t_1|t) \cong 1$ [Eq. (7)].

In order to check the validity of Eq. (35), we compare the analytical result to computer simulations of 2D and 3D phase transformations ruled by parabolic growth. In particular, for power growth laws and constant I_a Eq. (6) provides

$$\frac{d\xi(X_e)}{dX_e} = Dn \int_0^1 (1-\tau_1)^{Dn-1} P_c(t(X_e),\tau_1) d\tau_1, \tag{41}$$

which links the kinetics to the conditional probability $P_c(t|t_1)$. In Eq. (41) $t = t(X_e)$ is obtained through inversion of the $X_e = X_e(t)$ function and $\tau_1 = t_1/t$. Notably, a scaling argument applied to Eq. (10) reveals that for given nucleation and growth laws, $\xi = \xi(X_e)$ at $I_a = \text{const}$. The comparison between the analytical approach [Eqs. (35), (41)] and the numerical simulation is displayed in Fig. 8(a) for parabolic growth ($n = 1/2$) and indicates that the conditional probability computed here, retaining terms up to f_2, well describes the kinetics up to $\xi \cong 0.6$. Similar results have been obtained for the linear growth in Fig. 8(b), by means of Eqs. (40), (41) at $n = 1$ (solid symbols) and the KJMA formula (open symbols). The comparison between the analytical computation

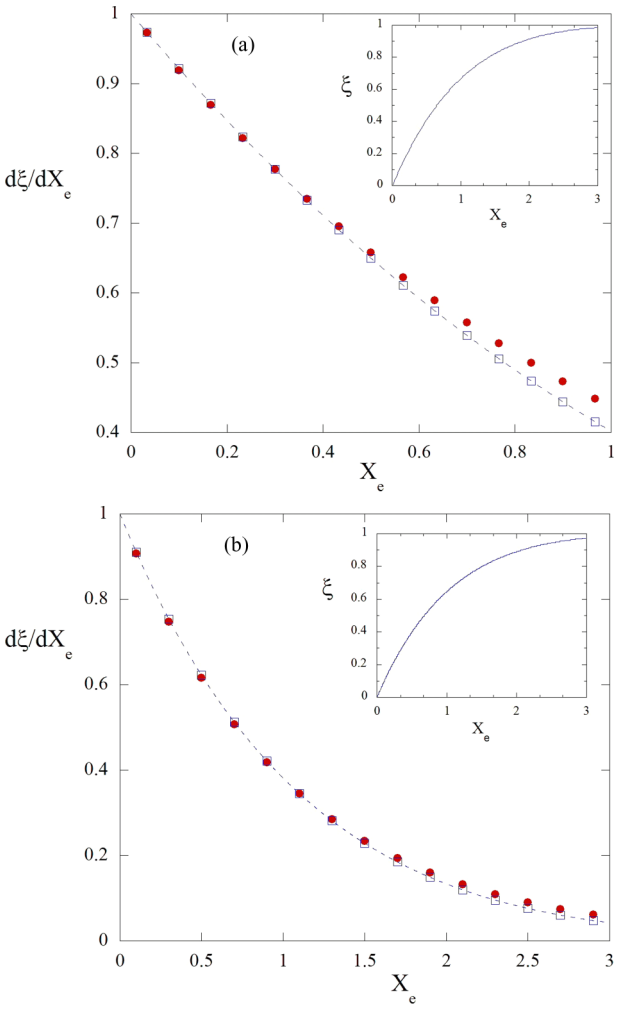

FIG. 9. (Color online) 3D phase transition. (a) Dimensionless rate $\frac{d\xi}{dX_e}$, computed using Eq. (41) and the $P_c(t|t_1)$ probability of Fig. 6, as a function of the extended volume for parabolic growth ($n = 1/2$) and constant value of the actual nucleation rate (solid symbols). The same quantity, as obtained by computer simulation, is also displayed (open symbols and dashed line). (b) Dimensionless rate $\frac{d\xi}{dX_e}$ for linear growth and constant value of the actual nucleation rate computed through Eq. (41) at $n = 1$ (solid symbols). The derivative of the kinetics obtained by computer simulation is displayed as open symbols and dashed line. The kinetics of the volume fraction $\xi(X_e)$ vs actual extended volume, are reported in the insets.

and the 3D simulations are reported in Figs. 9(a) and 9(b) for parabolic [Eqs. (35), (41)] and linear [Eqs. (40), (41)] growths, respectively. For $n = 1/2$ the results are similar to those attained for the 2D case while, for $n = 1$, the analytical approach is in very good agreement with the simulation in the entire range of the volume fraction.

Finally, we apply the theory to the case, widely considered in the literature, of constant value of the phantom-included nucleation rate, I_0. In this case the relation holds,

$$\frac{d\xi(\hat{X}_e)}{d\hat{X}_e} = Dn\int_0^1 (1-\tau_1)^{Dn-1}[1-\xi(\tau_1 t(\hat{X}_e))] \times P_c(t(\hat{X}_e),\tau_1)d\tau_1, \quad (42)$$

where $\hat{X}_e$ is the phantom-included extended surface (volume). The computation of $P_c(t|t_1)$ is carried out through numerical integration of Eq. (A11) (see the Appendix) where $I_a(t_2) = I_0[1-\xi(t_2)]$. To this end, we make use of the $\xi(\hat{X}_e)$ function available from computer simulations of 3D parabolic growth at $I_0 = \text{const}$ [33]. Once expressed in terms of the dimensionless variables τ_1 and $\hat{X}_e$, the argument of the exponential entering the probability $P_c \cong \exp(-\tilde{I}_1)$ [Eq. (A11)] becomes

$$\tilde{I}_1(\hat{X}_e,\tau_1) = (3n+1)\hat{X}_e\int_0^1 \left[(1-\tau_2)^{3n} - \frac{3}{4\pi}\varpi_3((1-\tau_2)^n, |\tau_1-\tau_2|^n; (1-\tau_1)^n)\right][1-\xi(t(\hat{X}_e)\tau_2)]d\tau_2, \quad (43)$$

where $t(\hat{X}_e) = (\frac{8\pi}{15}I_0 v^3)^{-2/5}\hat{X}_e^{2/5}$. The P_c function is further employed in Eq. (42) to evaluate the derivative of the volume fraction as a function of extended volume, $\hat{X}_e$. The result, displayed in Fig. 10(a), indicates that the theory is in very good agreement with the computer output in the whole range of volume fraction. Notably, also in the case of linear growth, $n = 1$, the theory is in very good agreement with the KJMA kinetics, as Fig. 10(b) shows. In this case $I_a(t_2) = I_0\exp[-\hat{X}_e(t)\tau_2^4]$. From the present analysis it stems that the truncation of the cluster expansion of P_c up to the f_2 term, works better at constant I_0, where the concentration of phantoms is actually very small [33]. On the other hand, a much larger number of phantoms is expected nucleating at $I_a = \text{const}$ rather than at $I_0 = \text{const}$. As a consequence, for $I_a = \text{const}$ the f_2-containing term gives a less accurate description of the whole kinetics for both 2D and 3D transitions (Figs. 8, 9).

B. Effect of the hard-core discontinuity on $P_c(t|t_1)$ and $q(t_1|t)$ functions

This section is devoted to analyzing the effect brought about by the non-continuous Heaviside function on the expression of the probability P_c reported above. In the following, the actual nucleation rate is taken as constant and only second-order terms are considered. To this end, the time derivative is performed after integration over the space variables. In fact, integration over the space variables gives the overlap area (volume) that is a continuous function. In the 2D case the $F_2(t_1,t_2;t)$ function becomes

$$F_2(t_1,t_2;t) = H(t_1-t_2)\int_0^{2\pi}d\theta_1\int_0^{R_{1t}} r_1 dr_1\left[\pi R_{2t}^2 - \varpi_2(R_{12},R_{2t};r_1)\right] + H(t_2-t_1)\int_0^{2\pi}d\theta_2\int_0^{R_{2t}} r_2 dr_2\left[\pi R_{1t}^2 - \varpi_2(R_{12},R_{1t};r_2)\right]. \quad (44)$$

The derivative of Eq. (44) is

$$\frac{\partial F_2}{\partial t} = \pi^2\partial_t\left(R_{1t}^2R_{2t}^2\right) - A(t_1,t_2;t)H(t_1-t_2) - A(t_2,t_1;t)H(t_2-t_1), \quad (45)$$

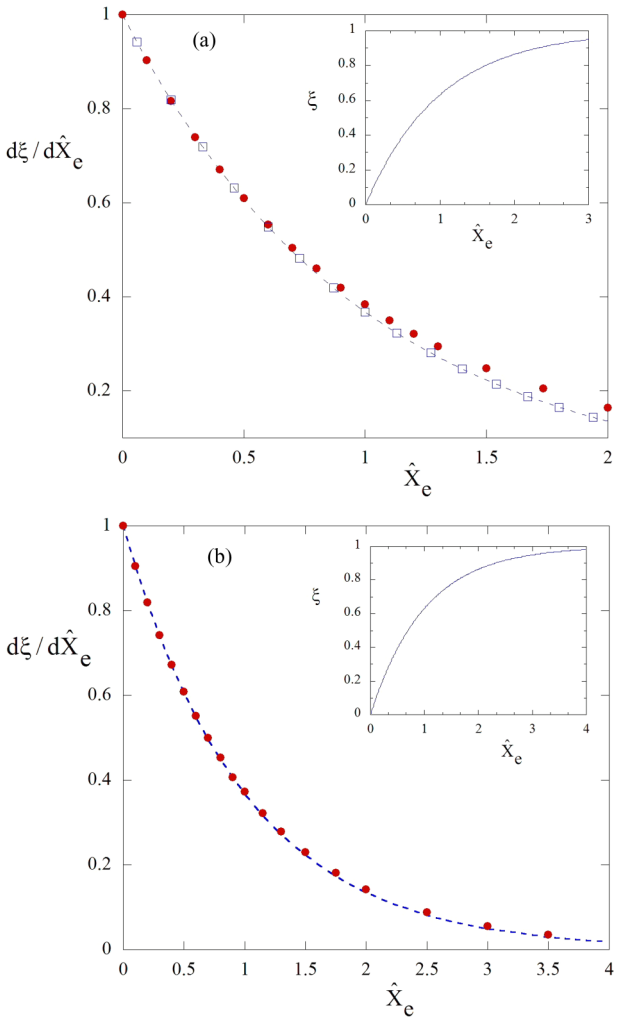

FIG. 10. (Color online) 3D phase transition. (a) Dimensionless rate $\frac{d\xi}{d\hat{X}_e}$, computed using Eqs. (42) and (43), as a function of the phantom-included extended volume ($\hat{X}_e$) for parabolic growth ($n = 1/2$) and constant value of I_0 (solid symbols). The same quantity, as obtained by computer simulation, is also displayed (open symbols and dashed line). (b) Dimensionless rate $\frac{d\xi}{d\hat{X}_e}$ for linear growth ($n = 1$) and constant value of I_0 computed through Eqs. (42) and (43) (solid symbols). The derivative of the KJMA kinetics is displayed as dashed line. The kinetics of the volume fraction $\xi(\hat{X}_e)$ vs $\hat{X}_e$ are reported in the insets.

where

$$A(t_1,t_2;t) = 2\pi\left[\varpi_2(R_{12},R_{2t};R_{1t})R_{1t}\partial_t R_{1t} + \int_{R_{2t}-R_{12}}^{R_{1t}} \partial_t\varpi_2(R_{12},R_{2t};x)x\,dx\right]$$
$$= 2\pi R_{1t}\partial_t R_{1t}\left[\varpi_2(R_{12},R_{2t};R_{1t}) + \frac{\partial_t R_{2t}}{R_{1t}\partial_t R_{1t}}\int_{R_{2t}-R_{12}}^{R_{1t}} \partial_{R_{2t}}\varpi_2(R_{12},R_{2t};x)x\,dx\right]. \quad (46)$$

Taking the time derivative of the transformed fraction [Eq. (10)] and using Eqs. (45), (46) together with the definition of P_c given by Eq. (6), we get

$$P_c(t|t_1) \cong 1 - X_e(t) + I_a\int_0^{t_1} dt_2\left[\varpi_2(R_{12},R_{2t};R_{1t}) + \frac{\partial_t R_{2t}}{R_{1t}\partial_t R_{1t}}\int_{R_{2t}-R_{12}}^{R_{1t}} \partial_{R_{2t}}\varpi_2(R_{12},R_{2t};x)x\,dx\right], \quad (47)$$

which is easily generalized to the 3D case according to

$$P_c(t|t_1) \cong 1 - X_e(t) + I_a\int_0^{t_1} dt_2\left[\varpi_3(R_{12},R_{2t};R_{1t}) + \frac{\partial_t R_{2t}}{R_{1t}^2\partial_t R_{1t}}\int_{R_{2t}-R_{12}}^{R_{1t}} \partial_{R_{2t}}\varpi_3(R_{12},R_{2t};x)x^2\,dx\right]. \quad (48)$$

In the case of parabolic growth law, using dimensionless variables one eventually obtains

$$P_c(t|t_1) \cong 1 - X_e(t)[1-\beta(\tau_1)],$$
$$q(t_1|t) \cong \frac{[1-X_e(t_1)]}{[1-X_e(t)]}\{1 - X_e(t)[1-\beta(\tau_1)]\}, \quad (49)$$

where

$$\beta(\tau_1) = \frac{(Dn+1)}{\pi^{D/2}}\Gamma(D/2+1) \times \int_0^{\tau_1} d\tau_2\left[\varpi_D((\tau_1-\tau_2)^{1/2},(1-\tau_2)^{1/2};(1-\tau_1)^{1/2}) + (1-\tau_2)^{-1/2}(1-\tau_1)^{1-D/2} \times \int_{(1-\tau_2)^{1/2}-(\tau_1-\tau_2)^{1/2}}^{(1-\tau_1)^{1/2}} \partial_{R'_{2t}}\varpi_D(\tau_1,\tau_2;x')x'^{D-1}dx'\right] \quad (50)$$

with $x' = x/vt^{1/2}$ and $R'_{2t} = R_{2t}/vt^{1/2} = \sqrt{1-\tau_2}$ being the dimensionless lengths. Comparison between Eqs. (35) and (49) indicates that in the low-coverage regime the effect of the boundary implies the presence of the $b(\tau_1)$ function in place of $\beta(\tau_1)$. In fact, since $\beta(\tau_1 \to 0) = 0$ and $\xi(t) \cong X_e$ for $X_e << 1$, Eq. (49) leads to the correct limit $P(t|0) = 1 - \xi(t)$. This limit is not well satisfied by Eq. (35), giving $b(0) = 0.125$ and 0.0625 for 2D and 3D growths, respectively. The $P_c(t|t_1)$ and $q(t_1|t)$ probabilities computed from Eqs. (49)–(50) are plotted in Fig. 11, as a function of the dimensionless time ($D = 2$). In the low coverage regime $q(t_1|t)$ is found to be, in fact, in agreement with the behavior of the kinetics reported in Fig. 7. In Figs. 12(a)–12(b) the functions $P_c(t|t_1)$ [see Eq. (49)] are compared to those obtained in the previous section on the ground of the cluster expansion, for both 2D and 3D growths. As far as the kinetics of the transformation is concerned, it is worth noting that, although the $P_c(t|t_1)$ curves are different, they lead to the same kinetics, i.e., to the same $d\xi/dX_e$ value. In other words, the edge effect does not play a significant role on the kinetics of the transformation which, according to Eq. (41), is linked to the $P_c(t|t_1)$ function through integration. It is this operation which reduces the effect of the function discontinuity on the kinetics.

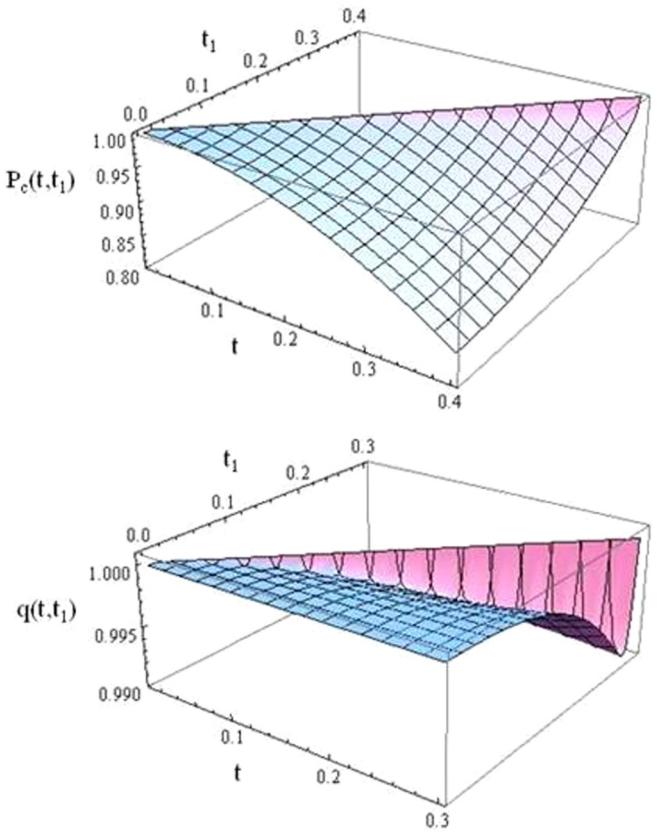

FIG. 11. (Color online) The $P_c(t|t_1)$ and $q(t_1|t)$ probabilities in the low-coverage regime for 2D parabolic growth and constant I_a. The computation—developed as discussed in Sec. III B—is not affected by the Heaviside discontinuity when performing the derivative of the transformed fraction. Please notice that the minimum of the q function is made visible because the scale has been magnified by a factor of about 100. Dimensionless variables t and t_1 are defined as in Fig. 5.

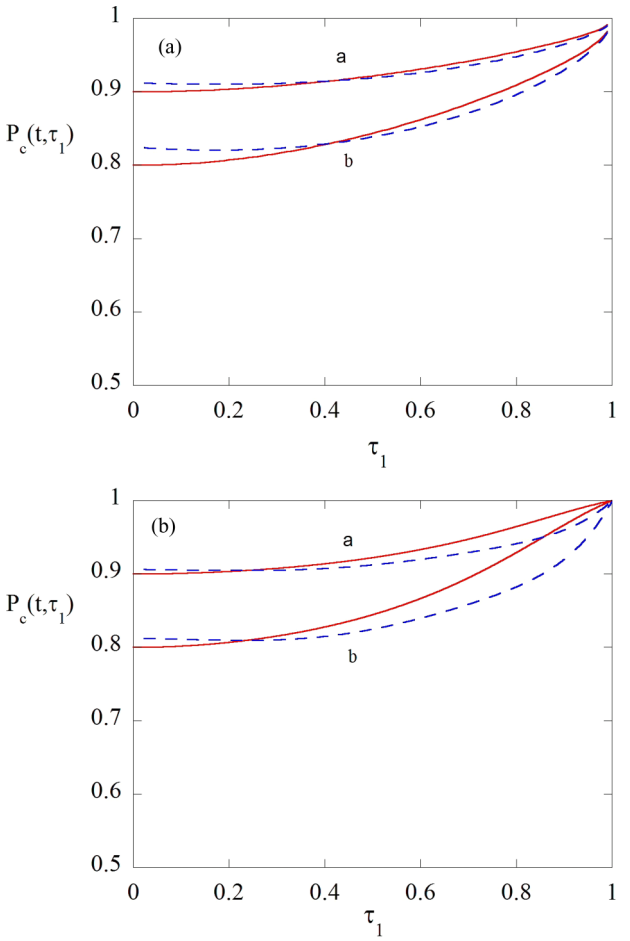

FIG. 12. (Color online) The $P_c(t|t_1)$ functions in the low-coverage regime computed from Eq. (49) at $X_e = 0.1$ (curve a, solid line) and $X_e = 0.2$ (curve b, solid line). (a) and (b) refer to 2D and 3D parabolic growths, respectively. The same quantity, computed using $b(\tau_1)$ in place of $\beta(\tau_1)$ in Eq. (49), is also reported as a dashed line.

Notably, for linear growth the effect of the boundary analyzed here vanishes. In fact, it is possible to show that the derivative Eq. (45) coincides with the expression obtained by performing the differentiation under the integral sign since, in Eq. (46), $R_{1t} = R_{2t} - R_{12}$ and $\varpi_D(R_{12}, R_{2t}; R_{1t}) = \frac{\pi^{D/2}}{\Gamma(D/2+1)} R_{12}^D H(t_1 - t_2)$.

Before concluding this section we apply the present calculation to estimate the last term in the square brackets of the differential equation for q [Eq. (26)]. Using Eqs. (44)–(46), in the low coverage regime the first correction to the Alekseechkin equation is found to be (see Appendix B for details) $\int_0^{t_1} dt_2 I_0(t_2)[(1-\xi(t_2)) - q(t_2|t_1)]\partial_{t_1}\varpi_D(R_{12}, R_{2t}; R_{1t})$, which equals zero in the limit $q(t'|t) = 1 - \xi(t')$, namely at the lowest order of approximation for q.

IV. CONCLUSIONS

In this article we have presented a comparative study on the "differential-critical-region" and "correlation-functions-based" methods for modeling the kinetics of phase transitions, with particular emphasis on the case of non-KJMA compliant growths. The connection between these methods has been established by computing the $P_c(t|t_1)$ and $q(t_1|t)$ conditional probabilities, namely, the key quantities of the differential-critical-region approach, in terms of correlation functions. The expression of P_c has been obtained by means of the cluster expansion technique, which improves the accuracy of the computation. The relationship between the $P_c(t|t_1)$ and $q(t_1|t)$ functions has also been established in Eq. (7), which allows us to evaluate the $q(t_1|t)$ probability. The $P_c(t|t_1)$ function, computed by retaining first-order terms in the $\tilde{g}_k$ expansion, leads to a good description of the kinetics obtained by 2D- and 3D-computer simulations of parabolic growth. The discontinuity of the Heaviside function is found to have a negligible effect on the kinetics of the phase transformation. In the case of non-KJMA compliant growths both approaches indicate that closed-form solutions for $q(t_1|t)$ cannot be achieved. It must be stressed, however, that for parabolic growth this result is only conceptually important, given the negligible effect of phantoms on the kinetics as scrutinized in previous works at $I_0 = \text{const}$ [26,33] and here at $I_a = \text{const}$.

Finally, the theory here developed can be applied to model phase transitions with spatially correlated nuclei and KJMA-compliant growth laws. Since in this case phantom overgrowth

is precluded the nucleation rate $I_0(t)$ can be employed in Eqs. (20), (23) in place of $I_a(t)$.

ACKNOWLEDGMENTS

The authors are indebted to Prof. R. Molle for the helpful discussions on the mathematical aspects of this work and to Dr. C. Hogan for the critical reading of the manuscript.

APPENDIX A: CLUSTER EXPANSION OF $P_c(t|t_1)$

We consider the following integral of Eq. (19):

$$\int_0^t dt_2 I_a(t_2)\cdots\int_0^t dt_m I_a(t_m)\int_{\Delta_{2t}} d\mathbf{r}_2\cdots \times\int_{\Delta_{mt}} d\mathbf{r}_m f_m(\mathbf{r}_1,\ldots,\mathbf{r}_m,t_1,\ldots,t_m)|_{\mathbf{r}_1=R_{1t}\hat{\mathbf{r}}_1}, \quad \text{(A1)}$$

where the f_m's depend upon $|\mathbf{r}_i-\mathbf{r}_j|$. Using relative coordinates, $\mathbf{x}_i=\mathbf{r}_i-R(t,t_1)\hat{\mathbf{r}}_1$, with $i>1$, the integral becomes

$$\begin{aligned}&\int_0^t dt_2 I_a(t_2)\cdots\int_0^t dt_m I_a(t_m)\int_{\Delta_{2t}} d\mathbf{x}_2\cdots \times\int_{\Delta_{mt}} d\mathbf{x}_m f_m(\mathbf{x}_2,\ldots,\mathbf{x}_m,t_1,\ldots,t_m)\\ &=\int_0^t dt_2 I_a(t_2)\cdots\int_0^t dt_m I_a(t_m)\int_{\Delta_{2t}} d\mathbf{x}_2\cdots \times\int_{\Delta_{mt}} d\mathbf{x}_m \bar{f}_{m-1}(\mathbf{x}_2,\ldots,\mathbf{x}_m,t_1,\ldots,t_m),\end{aligned} \quad \text{(A2)}$$

where $\bar{f}_{m-1}$ is a m-dots f-function. Changing the variable labels in Eq. (A2), the sum in Eq. (19) becomes

$$\begin{aligned}&\sum_{m=2}^{\infty}\frac{(-)^{m-1}}{(m-1)!}\int_0^t dt_2 I_a(t_2)\cdots\int_0^t dt_m I_a(t_m) \times\int_{\Delta_{2t}} d\mathbf{x}_2\cdots\int_{\Delta_{mt}} d\mathbf{x}_m \bar{f}_{m-1}(\mathbf{x}_2,\ldots,\mathbf{x}_m,t_1,\ldots,t_m)\\ &=\sum_{m=1}^{\infty}\frac{(-)^m}{m!}\int_0^t d\tau_1 I_a(\tau_1)\cdots\int_0^t d\tau_m I_a(\tau_m) \times\int_{\Delta_{1t}} d\mathbf{x}_1\cdots\int_{\Delta_{mt}} d\mathbf{x}_m \bar{f}_m(\mathbf{x}_1,\ldots,\mathbf{x}_m,t_1,\tau_1\ldots,\tau_m).\end{aligned} \quad \text{(A3)}$$

Next one defines a cluster expansion according to

$$\begin{aligned}\bar{f}_1(1)&=\tilde{g}_1(1),\\ \bar{f}_2(1,2)&=\tilde{g}_1(1)\tilde{g}_1(2)+\tilde{g}_2(1,2),\\ \bar{f}_3(1,2,3)&=\tilde{g}_1(1)\tilde{g}_1(2)\tilde{g}_1(3)+\tilde{g}_2(1,2)\tilde{g}_1(3)+\tilde{g}_2(1,3)\tilde{g}_1(2)\\ &\quad+\tilde{g}_2(2,3)\tilde{g}_1(1)+\tilde{g}_3(1,2,3),\end{aligned} \quad \text{(A4)}$$

and so on, where the numbers, in the argument of the functions, label the relative coordinates of nuclei. In particular, 1 stands for $\mathbf{x}_1=\mathbf{r}_2-R(t,t_1)\hat{\mathbf{r}}_1$, that is the relative coordinate of nucleus 2 with respect to nucleus 1.

The relationship between the $\tilde{g}_m$ and g_m functions can be expressed as

$$\begin{aligned}\tilde{g}_1(1)&=1+g_2(1),\\ \tilde{g}_2(1,2)&=g_3(1,2)+g_2(1,2)-g_2(1)g_2(2),\\ \tilde{g}_3(1,2,3)&=g_4(1,2,3)+g_3(1,2,3)-g_2(1)g_3(2,3)\\ &\quad-g_2(3)g_3(1,2)-g_2(2)g_3(1,3)\\ &\quad+2g_2(1)g_2(2)g_2(3),\end{aligned} \quad \text{(A5)}$$

and so on. In Eq. (A5) $g_3(1,2)\equiv g_3(\mathbf{x}_1,\mathbf{x}_2)$ is a three-dots correlation function, for nuclei 1,2,3, which is a function of the relative coordinates of nuclei 2 (i.e., $\mathbf{x}_1$) and 3 (i.e., $\mathbf{x}_2$), with respect to nucleus 1; also, $g_2(1,2)$ is a two-dots correlation function for nuclei 2 and 3 and $g_2(1)$ is a two-dots correlation function for nuclei 1 and 2.

Let us define the integral

$$\tilde{I}_k=\int_0^t d\tau_1 I_a(\tau_1)\cdots\int_0^t d\tau_k I_a(\tau_k)\int_{\Delta_{1t}} d\mathbf{x}_1\cdots \times\int_{\Delta_{kt}} d\mathbf{x}_k\tilde{g}_k(\mathbf{x}_1,\ldots,\mathbf{x}_k,t_1,\tau_1\ldots,\tau_k). \quad \text{(A6)}$$

The use of the cluster expansion Eq. (A4) allows one to decouple the integral [Eq. (A3)] in dependence of the multiplicity of the $\tilde{g}_m$ function. It follows:

$$\begin{aligned}&\int_0^t d\tau_1 I_a(\tau_1)\cdots\int_0^t d\tau_m I_a(\tau_m)\int_{\Delta_{1t}} d\mathbf{x}_1\cdots \times\int_{\Delta_{mt}} d\mathbf{x}_m \bar{f}_m(\mathbf{x}_1,\ldots,\mathbf{x}_m,t_1,\tau_1\ldots,\tau_m)\\ &=\sum_{n_1,n_2,\ldots,n_m}\frac{m!}{(1!)^{n_1}(2!)^{n_2}\ldots(m!)^{n_m}n_1!n_2!\ldots n_m!} \times(\tilde{I}_1)^{n_1}(\tilde{I}_2)^{n_2}\ldots(\tilde{I}_m)^{n_m},\end{aligned} \quad \text{(A7)}$$

where $\sum_{k=1}^m kn_k=m$. Using Eqs. (A3), (A7), Eq. (19) becomes

$$\begin{aligned}P_c(t|t_1)&=\sum_{n_1=0}^{\infty}\sum_{n_2=0}^{\infty}\cdots\sum_{n_m=0}^{\infty}\cdots\frac{(-)^{n_1}(\tilde{I}_1)^{n_1}}{(1!)^{n_1}n_1!}\frac{(-)^{2n_2}(\tilde{I}_2)^{n_2}}{(2!)^{n_2}n_2!}\ldots\\ &\quad\times\frac{(-)^{mn_m}(\tilde{I}_m)^{n_m}}{(m!)^{n_m}n_m!}\cdots\\ &=\exp\left[\sum_{m=1}^{\infty}\frac{(-)^m}{m!}\tilde{I}_m\right].\end{aligned} \quad \text{(A8)}$$

The first term in the argument of the exponential reads

$$\begin{aligned}\tilde{I}_1(t,t_1)&=\int_0^t d\tau_1 I_a(\tau_1)\int_{\Delta_{1t}} d\mathbf{x}_1\tilde{g}_1(\mathbf{x}_1,t_1,\tau_1)\\ &=\int_0^t dt_2 I_a(t_2)\int_{\Delta_{2t}} d\mathbf{x}_1 f_2(\mathbf{x}_1,t_1,t_2)\\ &=\int_0^t dt_2 I_a(t_2)\int_{\Delta_{2t}} d\mathbf{r}_2 f_2(\mathbf{r}_1,\mathbf{r}_2,t_1,t_2)|_{\mathbf{r}_1=R_{1t}\hat{\mathbf{r}}_1}.\end{aligned} \quad \text{(A9)}$$

Using the f_2 function given by Eq. (34), Eq. (A9) provides, eventually,

$$\tilde{I}_1(t,t_1) = \int_0^t dt_2 I_a(t_2)\left[\pi R_{2t}^2 - \varpi_2(R_{12},R_{2t};R_{1t})\right] \quad \text{(A10)}$$

for $2D$ growth and

$$\tilde{I}_1(t,t_1) = \int_0^t dt_2 I_a(t_2)\left[\frac{4\pi}{3}R_{2t}^3 - \varpi_3(R_{12},R_{2t};R_{1t})\right] \quad \text{(A11)}$$

for $3D$ growth, with the short notations $R(t_i,t) \equiv R_{it}$, $R(t_i,t_j) \equiv R_{ij}$. In Eqs. (A10), (A11), $\varpi_D(R_1,R_2;x)$ denotes the overlap area ($D=2$) and the overlap volume ($D=3$) of two nuclei of radius R_1 and R_2 at relative distance x (Fig. 2).

APPENDIX B: DIFFERENTIAL EQUATION FOR $q(t_1|t)$: PARABOLIC GROWTH

Expanding the argument of Eq. (15) up to g_2 gives rise to ($I = I_a$, 2D growth)

$$1-\xi = \exp\left[-\int_0^t dt_1 I_a(t_1)\pi R_{1t}^2 + \int_0^t dt_1 I_a(t_1) \times \int_0^{t_1} dt_2 I_a(t_2)(F_2(t_1,t_2,t) - \pi^2 R_{1t}^2 R_{2t}^2)\right], \quad \text{(B1)}$$

where F_2 is the integral over the space variables. Moreover,

$$\dot{\xi}(t) = [1-\xi(t)]\left[\int_0^t dt_1 I_a(t_1) 2\pi R_{1t}\partial_t R_{1t} - \int_0^t dt_1 I_a(t_1) \times \int_0^{t_1} dt_2 I_a(t_2)\partial_t\left(F_2 - \pi^2 R_{1t}^2 R_{2t}^2\right)\right], \quad \text{(B2)}$$

that is further elaborated by using Eqs. (45), (46), obtaining

$$\dot{\xi}(t) = [1-\xi(t)]\left\{\int_0^t dt_1 I_0(t_1)(1-\xi(t_1))2\pi R_{1t}\partial_t R_{1t} \times \left[1 + \int_0^{t_1} dt_2 I_a(t_2)\left(\varpi_2(R_{12},R_{2t};R_{1t}) + \frac{\partial_t R_{2t}}{R_{1t}\partial_t R_{1t}}\int_{R_{2t}-R_{12}}^{R_{1t}} \partial_{R_{2t}}\varpi_2(R_{12},R_{2t};x)x dx\right)\right]\right\}. \quad \text{(B3)}$$

The $q(t_1|t)$ function takes the form

$$q(t_1|t) = [1-\xi(t_1)]S^{(2)}(t_1,t), \quad \text{(B4)}$$

where $S^{(2)}$ is the last term in the square brackets of Eq. (B3).

In addition,

$$\partial_{t_1} S^{(2)} = \int_0^{t_1} dt_2 I_0(t_2)(1-\xi(t_2))\left[\partial_{t_1}\varpi_2 + \partial_{t_1} T(t_2,t_1,t)\right], \quad \text{(B5)}$$

with $T(t_2,t_1,t) = \frac{\partial_t R_{2t}}{R_{1t}\partial_t R_{1t}}\int_{R_{2t}-R_{12}}^{R_{1t}} \partial_{R_{2t}}\varpi_2(R_{12},R_{2t};x)x dx$.

The differential equation for $q(t_1|t)$ is eventually given by Eq. (26) according to

$$-\frac{\partial \ln q}{\partial t_1} \cong \int_0^{t_1} dt_2 q(t_2|t_1) I_0(t_2)\partial_{t_1}\omega_2 + \frac{1}{S^{(2)}}\int_0^{t_1} dt_2\left[q(t_2|t_1) - (1-\xi(t_2))\right] I_0(t_2)\partial_{t_1}\varpi_2 - \frac{1}{S^{(2)}}\int_0^{t_1} dt_2 I_0(t_2)(1-\xi(t_2))\partial_{t_1} T + O\left(I_0^2\right) \quad \text{(B6)}$$

which is the equation obtained by Alekseechkin [27] provided the terms normalized to $S^{(2)}$ are neglected. Equation (B6) can be easily generalized to the 3D growth.

[1] A. N. Kolmogorov, Bull. Acad. Sci. USSR (Cl. Sci. Math. Nat.) **3**, 355 (1937); *Selected Works of A. N. Kolmogorov*, edited by A. N. Shiryayev (Kluwer, Dordrecht, 1992), English translation, Vol. 2, p. 188.

[2] W. A. Johnson and R. F. Mehl, Trans. AIME **135**, 416 (1939).

[3] M. Avrami, J. Chem. Phys. **7**, 1103 (1939); **8**, 212 (1940).

[4] P. Bruna, D. Crespo, and R. González-Cinca, J. Appl. Phys. **100**, 054907 (2006).

[5] R. A. Ramos, P. A. Rikvold, and M. A. Novotny, Phys. Rev. B **59**, 9053 (1999).

[6] E. L. Rumyantsev, Ferroelectics **341**, 75 (2006).

[7] J. Farjas and P. Roura, Phys. Rev. B **75**, 184112 (2007); **78**, 144101 (2008).

[8] A. V. Teran, A. Bill, and R. B. Bergmann, Phys. Rev. B **81**, 075319 (2010).

[9] E. Bosco and S. K. Rangarajan, J. Chem. Soc. Faraday Trans. 1 **77**, 483 (1981); E. Budevski, G. Staikov, and W. J. Lorenz, *Electrochemical Phase Formation and Growth: an introduction to the initial stages of metal deposition* (VCH, New York/Basel/Cambridge/Tokyo, 1996).

[10] S. Jun, H. Zhang, and J. Bechhoefer, Phys. Rev. E **71**, 011908 (2005); S. Jun and J. Bechhoefer, *ibid.* **71**, 011909 (2005).

[11] M. Brits, W. Liebenberg, and M. M. de Villiers, J. Pharmaceutical Science **99**, 1138 (2010).

[12] C. Greenwood, K. Rogers, S. Beckett, and J. Clement, J. of Materials Science: Materials in Medicine **23**, 2055 (2012).

[13] M. P. Shepilov and D. S. Baik, J. Non. Cryst. Solids **171**, 141 (1996).

[14] B. J. Kooi, Phys. Rev. B **70**, 224108 (2004).

[15] D. P. Birnie III and M. C. Weinberg, J. Chem. Phys. **103**, 3742 (1995).

[16] S. J. Song, F. Liu, Y. H. Jiang, and H. F. Wang, Acta Materialia **59**, 3276 (2011).

[17] A. A. Burbelko, E. Fraś, and W. Kfapturkiewicz, Mater. Sci. and Eng. A **413–414**, 429 (2005).

[18] E. Pineda, T. Pradell, and D. Crespo, Phil. Mag. A **82**, 107 (2002).

[19] M. Fanfoni, M. Tomellini, and M. Volpe, Phys. Rev. B **65**, 172301 (2002).

[20] B. Petukhov, J. Stat. Mech.: Theor. Exp. (2013) P09019.
[21] A. Korobov, Phys. Rev. B **76**, 085430 (2007).
[22] N. V. Alekseechkin, J. of Physics: Condens. Matter **12**, 9109 (2000).
[23] M. Fanfoni and M. Tomellini, Il Nuovo Cimento **20D**, 1171 (1998).
[24] M. Tomellini and M. Fanfoni, Phys. Rev. B **78**, 014206 (2008).
[25] M. Tomellini and M. Fanfoni, Phys. Rev. B **55**, 14071 (1997).
[26] M. P. Shepilov, Crystallography Reports **50**, 513 (2005).
[27] N. V. Alekseechkin, J. Non Cryst. Solids **357**, 3159 (2011).
[28] M. Tomellini and M. Fanfoni, Phys. Rev. E **85**, 021606 (2012).
[29] It is worth noticing that changing the integration variable from t_1 to r in Eq. (8) one obtains the expression employed in [26] for estimating the contribution of phantoms in diffusional growth.
[30] M. Fanfoni and M. Tomellini, Eur. Phys. J. B **34**, 331 (2003).
[31] M. Fanfoni and M. Tomellini, J. Phys.: Cond. Matter **17**, R571 (2005).
[32] T. Hill, *Statistical Mechanics* (Dover, New York, 1987).
[33] E. Pineda and D. Crespo, Phys. Rev. B **60**, 3104 (1999)